Transition from Absolute to Convective Instability in a Beam-Plasma System*

D. Boyd, W. Carr, J. Manickam, B. Rosen, and M. Seidl
Stevens Institute of Technology, Hoboken, New Jersey 07030
(Received 19 April 1972; revised manuscript received 26 April 1973)

The electrostatic instability in a magnetoplasma, $\omega > \omega_{ce}$, excited by a weak electron beam is found to be either convectively unstable (amplifying) or absolutely unstable (oscillating) depending upon effective plasma electron temperature and beam density. Measurements of the transition between the two types agree with calculations.

In this Letter we present results of the investigation of the electrostatic instability in a magnetoplasma excited by a weak longitudinal beam with $\omega > \omega_{ce}$, $\omega \simeq k_z V$, the H^0 wave.[1] We find that this may be made either absolutely or convectively unstable by adjustment of system parameters, which permits a direct comparison between these types in a single experimental geometry. The experimentally observed instabilities differ in both linear and nonlinear properties. Here we will discuss the linear regime; results of the nonlinear measurements will be published later.

It has been shown theoretically that this mode is absolutely unstable for a cold plasma,[2] although this has not been clearly established experimentally. Recent experiments[3,4] do not discuss the possibility. In this experiment we have found that the mode is absolutely unstable when the plasma is effectively cold enough, but it becomes convectively unstable at modest temperature.

We have measured the dispersion relation in the two cases and examined the dependence of the transition between them on system parameters. The results are compared with the dispersion equation given by

$$\epsilon(k, \omega) = 1 + \kappa_P + \kappa_B = 0, \tag{1}$$

where

$$\kappa_P = \frac{2\omega_P^2}{k^2 v_t^2}\left[1 + \frac{\omega}{|k_z| v_t} \sum_{n=-\infty}^{+\infty} Z\left(\frac{\omega - n\omega_c}{|k_z| v_t}\right) e^{-\lambda} I_n(\lambda)\right]$$

and

$$\kappa_B = -\frac{R\omega_B^2}{(\omega - k_z V)^2}\frac{k_z^2}{k^2}.$$

ω_P, ω_B, and ω_c are the plasma frequency, beam plasma frequency, and electron cyclotron frequency, respectively, v_t is the electron thermal velocity in the plasma, $\lambda = k_\perp^2 v_t^2/2\omega_c^2$, Z is the plasma dispersion function, V is the beam velocity, I_n is the nth-order modified Bessel function, and $k^2 = k_\perp^2 + k_z^2$. The potential is assumed to have the form $J_0(k_\perp r)\exp[i(k_z z - \omega t)]$ and thus the propagation is axial, with $k_\perp$ determined by transverse geometry. R is the beam reduction factor which is included to take into account the fact that the beam has a smaller diameter than the plasma. $\omega_B R^{1/2}$ is thus an effective plasma frequency of the beam.[5]

The experimental configuration and measurement techniques are described elsewhere.[6] The plasma, produced by a dc discharge in He, with trace Ar, is 85-cm long and 3 cm in diameter. A longitudinal electron beam of 5-mm diam is coaxial with the plasma; the axis of the system is along the uniform magnetic field. The waves propagate axially with a radius of 3 mm, which is comparable to the beam radius. The numerical values of the experimental parameters are given with the experimental results.

The two types of instability behave very differently. The convective wave has the well-known properties; a small perturbation applied near the gun is spatially amplified and saturates, the amplitude pattern being steady in time. Linear growth rates have $\mathrm{Im}(k_z)/\mathrm{Re}(k_z) \lesssim 0.1$ for beam densities used. Spatial growth is found everywhere within the unstable region.

The absolute instability oscillates at essentially a single frequency; it occurs spontaneously and cannot be launched or synchronized by external modulation. It does not have an exponential growth in space; near the electron gun it rises from zero to maximum amplitude very quickly (< 2 wavelengths), then decays slowly in space. The amplitude is usually not steady in time, but switches off and on in time intervals of 0.1 to 10 μsec. Off-to-on amplitude ratios as high as 50 dB have been observed.

We have measured the propagation constants in the absolute and convective regimes, with the results shown in Figs. 1 and 2. Experimental

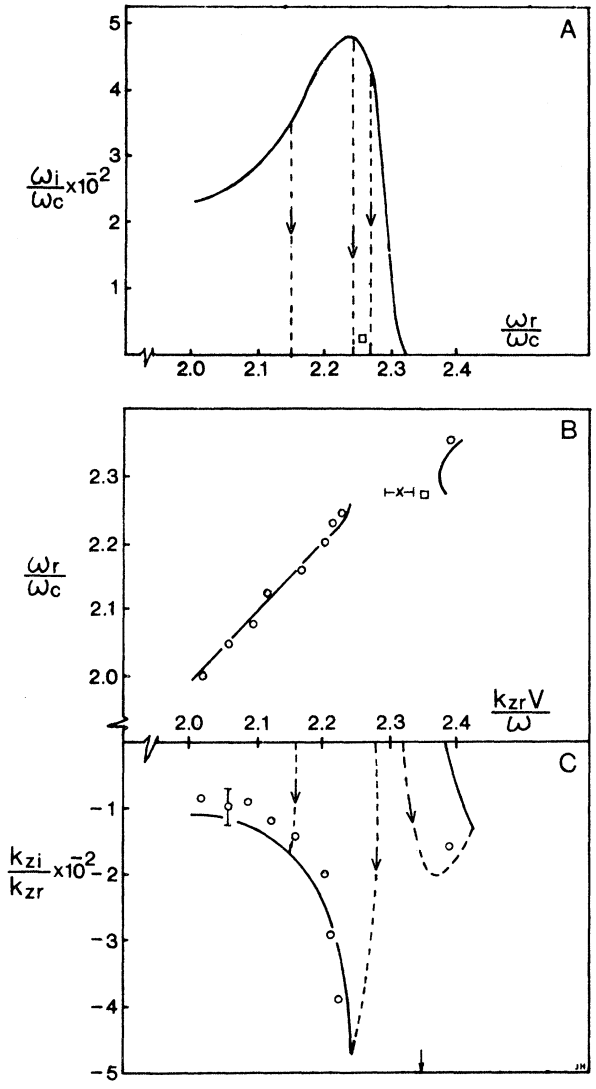

FIG. 1. Measured and calculated propagation constants for absolute instability. Solid curves and squares, theory; circles and cross, experiment; dashed lines, typical trajectories in mapping. (a) Theory for real k_z, complex ω. (b) ω versus k_z after mapping. Circles are for launched waves and the cross is for oscillations. (c) Complex k_z plane after mapping. The theory gives a saddle point beyond the graph indicated by the arrow.

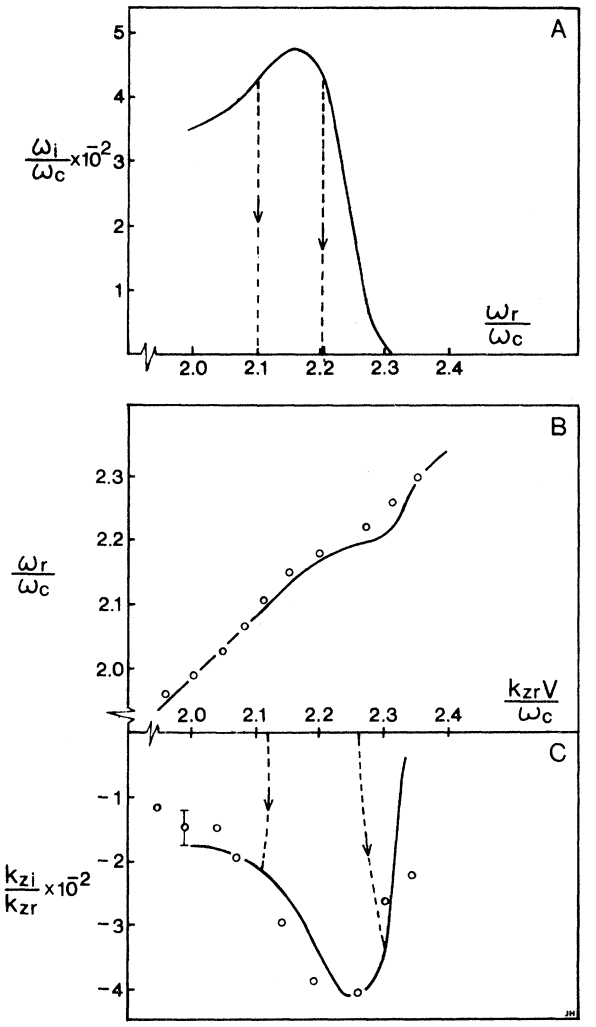

FIG. 2. Measured and calculated propagation constants for convective instability. The plotting conventions are those of Fig. 1. (a) Theory for real k_z, complex ω; (b) ω versus k_z after the mapping; (c) k_z plane after mapping.

data are plotted as open circles for launched waves and a cross for the spontaneous oscillation. Also shown are the results of the calculation, given by the lines and squares. In Fig. 1 the system was adjusted so that the oscillation is present. The experimental parameters are as follows: $\omega_c = 3.3\times10^9$ sec^{-1}, $\omega_p = 6.5\times10^9$ sec^{-1}, $\omega_B = 7.3\times10^7$ sec^{-1}, $v_t = 6.6\times10^7$ cm/sec, and $V = 1.1\times10^9$ cm/sec. To obtain the data in Fig. 2 the beam velocity is reduced to $V = 9.3\times10^8$ cm/sec with all other parameters held constant. This causes the oscillation to disappear and spatial growth is observed throughout the band.

The curves in Figs. 1 and 2 were calculated from (1) using the Bers-Briggs[7] mapping which identifies the absolute instability and gives the spatial solutions. The factors in (1) were evaluated by directly substituting the experimental constants given above, and only V is changed in going from Fig. 1 to Fig. 2. In addition, the fixed constants $R = \frac{1}{4}$ and $k_\perp = 10$ cm^{-1} were obtained by fitting the experimental data in Fig. 2. The values of R and $k_\perp$ thus obtained are in approximate agreement with a calculation which self-consistently includes radial boundary condi-

tions. The results of the calculation will be published elsewhere.

The calculation follows Briggs.[7] In both cases (1) is solved for real k_z, resulting in complex ω roots with $\mathrm{Im}(\omega) > 0$ which implies that the mode is unstable[8] [curves in Figs. 1(a) and 2(a)]. Then $\mathrm{Im}(\omega)$ is reduced to zero with $\mathrm{Re}(\omega)$ fixed. Solutions $k = k(\omega)$ are traced out in the k_z plane, and typical trajectories of the roots are shown by dashed lines. The results of the mapping are given by the curves in Figs. 1(c) and 2(c). The curves in Figs. 1(b) and 2(b) relate $\mathrm{Re}(\omega)$ to $\mathrm{Re}(k_z)$ after the mapping; Fig. 1(b), 1(c), 2(b), and 2(c) are thus for the spatial case corresponding to the experiment. In Fig. 2 the mapping is continuous, thus the instability is convective. There is a branch point in the ω plane, indicated by the box in Fig. 1, and thus the continuous curve in ω is mapped into two branches in the k plane. There is a saddle point in k off scale at the arrow. According to the Bers-Briggs criteria Fig. 1 shows absolute instability.

For the convective instability, Fig. 2, both theory and experiment give spatially growing waves throughout the unstable band, while for the absolute instability, Fig. 1, both exhibit a gap in the center of the band where spatially growing waves do not exist. The oscillation which is found in the experiment clearly corresponds to the singularity of the calculations.

When V is increased beyond that of Fig. 1, the stop band for amplified waves broadens until amplified waves are no longer observed. This absence of amplified waves could be used to define "pure" absolute instability; however, we follow the theoretical definition of Briggs, and define absolute instability as the existence of the oscillation.

In both cases the agreement between theory and experiment is good. Therefore we consider that (1) provides an adequate description of the experiment, and the transverse geometry is well approximated by fixed R and $k_\perp$.

In the theory the linear properties of the absolute instability are given by the ω and k_z coordinates of the branch point and saddle point. The oscillation should thus have these values, and the linear wave should be growing in time. However, the experiment is steady state, which implies that the observed oscillation is saturated. We have made no systematic study of the transient behavior; however, an estimate of the temporal growth rate of the oscillation was made using the pulsed behavior mentioned previously. This yields a value $\mathrm{Im}(\omega)/\mathrm{Re}(\omega) \simeq 0.01$, which is in order of magnitude agreement with the calculation.

The results in Figs. 1 and 2 show a transition from absolute to convective instability as the beam voltage is reduced. We have also studied the dependence of the transition upon other parameters. We have observed the transition by changing the plasma electron temperature, through adjustment of the discharge conditions. We have studied the dependence on ω_B and ω_c, with results shown in Fig. 3.

The solid and dashed curves are calculated, using the values of ω_c given, by solving (1) with the constraint that the branch point has $\mathrm{Im}(\omega) = 0$. The experimental points are obtained by increasing the beam density from a low value, where the oscillation is absent, to the point where the oscillation appears. This is repeated for various values of ω_P and ω_c, as shown. Beyond $\omega \simeq 2.5\omega_c$ the beam electron gun is heated by the plasma so that threshold measurements could not be taken above this point.

Our physical interpretation of these results is that the transition depends upon the beam density and the effective plasma temperature. From (1), the plasma is effectively cold when $k_\perp v_t/\omega_c \ll 1$ and $(\omega - n\omega_c)/k_z v_t \simeq (1 - n\omega_c/\omega)V/v_t \gg 1$. At fixed temperature, the beam must exceed a critical density in order to overcome the plasma loss and

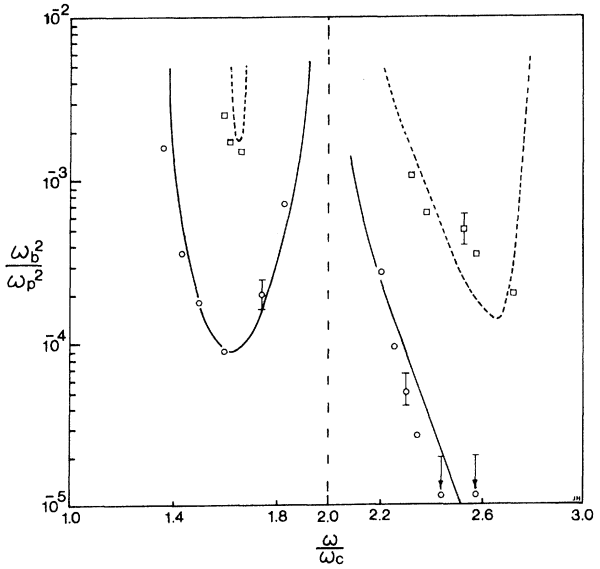

FIG. 3. Threshold for absolute instability. Theoretical curves are calculated using the experimental values $\omega_c = 3\times10^9$ sec^{-1} for the solid curves and $\omega_c = 4.8\times10^9$ sec^{-1} for the dashed curves. The absolute instability exists above the threshold curve in each case.

drive the oscillation, and this threshold density increases with increasing temperature. At fixed beam density the instability will become convective when the plasma is made effectively warmer, since the given density will become smaller than the threshold value. The experimental results are thus due to the changes in threshold beam density in response to changes in the thermal parameters. In Figs. 1 and 2 v_t/V is changed, and in Fig. 3 the threshold increases as $k_\perp v_t/\omega_c$ increases and also as ω approaches $n\omega_c$, where $\omega - n\omega_c \simeq 0$.

In this experiment the plasma can be made effectively warm enough so that we have convective instability at the maximum attainable beam density ($\omega_B^2/\omega_P^2 \simeq 10^{-2}$). In terms of thermal parameters this occurs when $k_\perp v_t/\omega_c > 0.1$ and $V/v_t < 10$.

From this work we conclude that plasma thermal effects must be considered in the analysis of H-wave experiments, since either convective or absolute instability may be present. We have examined experiments on the H wave by other workers, and conclude that the observed waves were absolute instabilities[3,9,10] except for the work of Mizuno and Tanaka.[4] There the cold-plasma dispersion relation was erroneously used to describe a convective instability.

*Work supported by the National Science Foundation and the U. S. Air Force Office of Scientific Research.

[1]M. Seidl, Phys. Fluids 13, 966 (1970).

[2]R. J. Briggs, *Electron-Stream Interactions with Plasmas* (Massachusetts Institute of Technology Press, Cambridge, Mass., 1964), p. 165.

[3]J. H. A. van Wakeren and H. J. Hopman, Phys. Rev. Lett. 28, 285 (1972).

[4]K. Mizuno and S. Tanaka, Phys. Rev. Lett. 29, 45 (1972).

[5]Briggs, Ref. 2, p. 101.

[6]W. Carr, D. Boyd, H. Liu, G. Schmidt, and M. Seidl, Phys. Rev. Lett. 28, 662 (1972).

[7]Briggs, Ref. 2, p. 30.

[8]Im(ω) and Im(k) have signs opposite to those of Ref. 7, since there the wave is of the form $\exp[i(\omega t - k_z z)]$.

[9]I. F. Kharchenko *et al.*, Zh. Tekh. Fiz. 34, 1031 (1964) [Sov. Phys. Tech. Phys. 9, 798 (1964)]; M. Seidl and P. Sunka, Nucl. Fusion 7, 237 (1967); T. Idehara, J. Phys. Soc. Jap. 23, 660 (1967).

[10]V. Piffl *et al.*, in *Proceedings of the Fourth International Conference on Plasma Physics and Controlled Nuclear Fusion Research, Madison, Wisconsin, 1971* (International Atomic Energy Agency, Vienna, 1972), Vol. II, p. 733.

Evolution of Bernstein-Greene-Kruskal–like Ion Modes with Trapped Electrons

A. Y. Wong, B. H. Quon, and B. H. Ripin
Department of Physics, University of California, Los Angeles, California 90024
(Received 20 April 1973)

The growth of an ion acoustic instability caused by a slow electron drift is studied experimentally. A small-amplitude test wave in this unstable system develops into a large-amplitude steady state which is found to be a Bernstein-Greene-Kruskal–like ion mode with trapped electrons.

We wish to report experimental observations of the spatial growth of ion acoustic waves in the presence of a slow electron drift.[1] The final state of the wave, which does not decay spatially, together with the measured distribution function, appear to be consistent with Bernstein-Greene-Kruskal (BGK) modes[2] with trapped electrons. Although theoretically predicted,[2] such modes have not been observed experimentally. The temporal or spatial evolution of such BGK modes have not been studied extensively either, presumably because of a lack of experimental evidence.

In our experiments we have chosen experimental parameters (density, temperature, and neutral pressures) such that electrons can execute many bounces in the ion acoustic wave potential well within a collisional time. For either ions trapped in ion waves[3] or electrons trapped in electron waves,[4,5] the bounce time of the trapped particles is usually slower than the wave period and it is difficult to observe experimentally steady-state or quasi–steady-state behavior. However, the large electron-to-ion temperature ratio ($T_e/T_i \approx 15$) and the high phase velocity of the ion acoustic wave favor the trapping of electrons rather than ions in our experiment. In order to facilitate the identification of trapped